Intern. J. Environ. Anal. Chem.
Vol. 90, No. 9, 10 August 2010, 747–759

Taylor & Francis
Taylor & Francis Group

Nanoelectrode ensembles for the direct voltammetric determination of trace iodide in water

Paolo Ugo[a]*, Ligia M. Moretto[a], Morena Silvestrini[a] and Francisco C. Pereira[b]

[a]*Department of Physical Chemistry, University of Venice, Calle Larga Santa Marta 2137, I-30123 Venezia, Italy;* [b]*Department of Chemistry, Federal University of Rio Grande do Norte, 59072-970 – Natal, RN, Brazil*

(*Received 28 November 2008; final version received 31 March 2009*)

Procedures for the preparation and characterisation of ensembles of gold nanodisk electrodes (NEE) of 30 nm diameter are presented, in particular focusing on improvements in the signal/background current ratios and detection limits with respect to the electrochemical oxidation of iodide and its analytical determination in water samples. At NEEs iodide undergoes a quasi-reversible diffusion controlled oxidation with a slight shift in $E_{1/2}$ values and slightly higher peak to peak separation with respect to conventional gold disk electrodes. The double layer charging current at the NEE is significantly lower than at conventional electrodes so that the detection limit (DL) by cyclic voltammetry with NEEs in tap water is significantly lower than DL at the Au-disk millimetre-sized electrode (DL 0.3 μM at NEE vs. 4 μM for Au-disk). Finally, it is shown that NEEs in combination with square wave voltammetry can be applied for the direct determination of iodide in water samples from the lagoon of Venice, with a detection limit of 0.10 μM.

Keywords: nanoelectrode ensembles; iodide; voltammetry; water analysis; lagoon water

1. Introduction

Iodine is an essential component required by the thyroid gland to produce two iodised hormones, thyroxine and tri-iodothyronine, which are used by the body during metabolism. The human body does not need much iodine and, on average, it contains around 20–25 mg of the element. When starved for iodine, the thyroid gland swells and this causes goitre.

Iodine is a trace element present in seawater and sea products, mainly in the form of iodide or iodate anions [1]. The most common sources of iodine intake for human beings are table salt and seafood, but also plants grown in iodine rich soils. Problems arise in certain parts of the world where the soil contain no iodine; this causes iodine deficiencies in the diet and consequent health problems [2,3].

Various methods have been proposed for iodide determination such as spectrophotometry [4], ICP-MS [5], capillary electrophoresis [6,7], ion-chromatography and HPLC [8–10], the latter being probably the most widely used.

*Corresponding author. Email: ugo@unive.it

ISSN 0306-7319 print/ISSN 1029-0397 online

DOI: 10.1080/03067310902962569
http://www.informaworld.com

By taking advantage of the electroactivity of iodide, electrochemical methods have been often applied to this goal, in particular cathodic stripping methods, following electrolytic pre-concentration of iodide in the form of insoluble salts deposited on the surface of a suitable electrode material, typically mercury or silver [11–14], but also at modified electrodes [15,16]. However, from the viewpoint of quick analytical control in the environment, direct methods (which could avoid a pre-concentration step) might be preferable.

Recent studies [17–22] showed that the use of the so-called nanoelectrode ensembles (NEEs), can improve the performances of electrochemical determinations, thanks to dramatically higher signal to background current ratios with respect to other electrode systems and this was demonstrated also in relation to the direct determination of iodide with NEEs [23].

The NEEs used in our laboratory are prepared by electroless deposition of gold electrode elements within the pores of a microporous track-etch polycarbonate membrane [24]. The diameter and length of the pores in the template determine the geometrical characteristics of the metal nanostructure, with radii as small as 30 nm. The introduction of the use of pre-formed microporous membranes as template for the synthesis of nanomaterials [21] was somehow revolutionary since it made accessible to almost any laboratory a simple but effective procedure for the easy preparation of nanomaterials. What is needed for the membrane based synthesis of nanomaterials is, in fact, very simple apparatus, such as apparatus for metal deposition and basic electrochemical instrumentation.

In the present work, we examine the use of NEEs for the direct electroanalysis of iodide in water samples, comparing the analytical performances of NEEs with conventional gold-disk electrodes also in waters from the marine environment, such as lagoon waters.

2. Experimental

2.1 *Materials*

Polycarbonate filtration membranes (SPI-Pore, 47 mm filter diameter, 6 μm filter thickness) with a nominal pore diameter of 30 nm and coated with the wetting agent polyvinyl-pyrrolidone were used as the templates to prepare the NEEs. Commercial gold electroless plating solution (Oromerse Part B, Technic Inc.) was diluted (40 times with water) prior to use.

All other reagents were of analytical grade and were used as received. Purified water was obtained using a Milli-Ro plus Milli-Q(Millipore) water purification system.

2.2 *Electrochemical measurements and instrumentation*

All electroanalytical measurements were carried out at room temperature (22 ± 1°C) using a three-electrodes single-compartment cell equipped with a platinum coil counter electrode and an Ag/AgCl (KCl saturated) reference electrode. All potential values are referred to this reference electrode. Voltammetric measurements with NEEs and Au electrodes were performed with a CH-660A (CHI-IJ Cambria Scientific, UK) instrument controlled by its own software. Cathodic stripping measurements at the hanging mercury drop electrode (HMDE) were performed using the EG&G Parc model 303A Static Mercury Drop Electrode in conjunction with an EG&G Parc model 394 Electromechanical Trace

Analyzer, controlled by its own software. In this case, the sample solutions were carefully degassed by bubbling nitrogen before each measurement.

2.3 *Electrode preparation*

The nanoelectrode ensembles were prepared using the electroless plating procedure described previously [21] and following modifications. In particular, the method described in references [24] and [25] was followed. Briefly, after wetting for 2 h in methanol, the polycarbonate template membrane was sensitised with Sn^{2+} by immersion into a solution that was 0.026 M in $SnCl_2$ and 0.07 M in trifluoroacetic acid in 50 : 50 methanol-water for 5 minutes. After rinsing with methanol for 5 min, the sensitised membrane was immersed for 10 min in 0.029 M $Ag[(NH_3)_2]NO_3$. The membrane was then immersed into the Au plating bath which was 7.9×10^{-3} M in $Na_3Au(SO_3)_2$, 0.127 M in Na_2SO_3. After waiting 30 minutes, 0.625 M formaldehyde was added to the plating bath; this delay time was introduced here since it allows one to separate the formation of the first gold nuclei (produced by galvanic displacement of metallic Ag° nuclei with Au° nuclei) from the following catalytic growth of these nuclei by further gold deposition caused by formaldehyde. The temperature of the bath was 0–2°C. Electroless deposition was allowed to proceed for 15 hours, after which additional 0.3 M formaldehyde was added. Deposition was continued for another 9 hours, after which the membrane was rinsed with water and immersed in 10% HNO_3 for 12 hours. The membrane was then rinsed again with water and dried. The final assembly of the NEE (for obtaining electrodes handy for use in an electrochemical cell) followed substantially the previous method [21], however slightly modifying the final assembly in that the copper tape which acts as electrical connection for the NEE was attached to the lower gold layer which completely covers one face of the membrane, instead of being attached to the upper gold layer as was previously done [21]. This modification improved the electrical connection between copper and the NEE.

The geometric area, A_{geom}, of the NEE (0.07 cm^2) is determined by the diameter (3 mm) of a hole punched in the insulating film (Monokote by Topflite) that covers the upper face (peeled) of the NEE. The average diameter of the nanodisks in these NEEs was measured by SEM and is 50 ± 10 nm [18].

Conventional millimetre-sized gold disk electrodes were prepared from a golden glass plate (thickness 1 mm) coated with nickel 80 Å, chromium 20 Å and gold 3900 Å on the outer surface. They were purchased from ACM France. The golden plate was cut into slides (ca. 2.5 cm × 1.0 cm) and the geometric area of the electrodes (0.07 cm^2) was defined, as it was made for the NEE, by the diameter of a hole punched in a strip of insulating tape which covers all the golden surface apart from the hole. The electrical contact was made with a copper tape before placing the insulating tape.

Before each set of measurements, the surface of the Au-disk electrode and NEEs was cleaned electrochemically by cycling in 0.5 M H_2SO_4 between −0.1 V and 1.5 V at 100 mV s^{-1}.

2.4 *Lagoon water samples*

Lagoon waters were collected sampling at about 25 cm depth in preconditioned bottles, in the north area of the Venice lagoon, close to Lido portal, where the waters present

an average salinity of 34 ‰ and pH 8.0. Samples were filtered through 0.45 μm Millipore membrane and acidified to pH 1 with some drops of sulphuric acid.

3. Results and discussion

3.1 *Preliminary considerations*

NEEs can be considered as ensembles of disc ultramicroelectrodes separated by an electrical insulator interposed between them. An ultramicroelectrode is considered as an electrode with at least one dimension comparable or lower than the thickness of the diffusion layer (typically $<25\,\mu m$). At such small electrodes, edge effects from the electrode become relevant and diffusion from the bulk solution to the electrode surface is described in terms of radial geometry instead of the simpler linear geometry used for larger ($>100\,\mu m$) electrodes. An NEE can be considered as a very large assembly of very small ultramicrolectrodes confined in a rather small space. Since the number of nanodiscs elements per unit surface of the ensemble is large (in our case 6.5×10^8 nanodisks cm^{-2} [18]), all the nanoelectrodes are statistically equivalent and the different contribution of the elements at the outer range of the ensemble can be considered negligible [19,26].

With respect to diffusing redox analytes, NEEs can exhibit two limit voltammetric response regimes which are ruled by the scan rate and/or by the reciprocal distance between the nanoelectrode elements [27]. When radial diffusion boundary layers overlap totally (radius of diffusion hemisphere larger than average hemi-distance between electrodes and/or slow scan rates) NEEs behave as planar macroelectrodes with respect to Faradaic currents (total overlap conditions, see Figure 1a).

When diffusion hemispheres become shorter than the hemi-distance between the nanoelectrodes (larger distance between the nanodisks and/or higher scan rates), the current response is dominated by radial diffusion at each single element; under these conditions, the pure radial regime is achieved (see Figure 1b). Really at very high scan rates, a so-called linear active regime can be reached [20]; however, this regime is not encountered commonly in the experimental practice, apart for recessed electrodes. Being characterised by the highest signal/background current ratios (see below), the total overlap and pure radial regimes are the regimes typically used for analytical and sensing applications.

Because of the geometrical characteristics, using NEEs obtained by commercial track-etched membranes as templates, the prevailing diffusion regime is the total overlap regime [20,21]. Transition from total overlap to the pure radial control as a function of nanoelements distance or scan rate was demonstrated experimentally by Martin and co-workers using specially made membranes [27] and by Ugo and co-workers with commercial membranes, but operating in high viscosity media [28].

Under total overlap diffusion regime, NEEs show enhanced electroanalytical detection limits, relative to a conventional millimetre-sized electrode. This is because the Faradaic current (I_F) at the NEE is proportional to the total geometric area (A_{geom}, nanodiscs plus insulator area) of the ensemble, while the double-layer charging current (I_C) is proportional only to the area of the electrode elements (active area, A_{act}) [21].

Faradaic-to-capacitive currents at NEEs and conventional electrodes with the same geometric area are related by Equation (1) [20,21]:

$$(I_F/I_C)_{NEE} = (I_F/I_C)_{conv}\, A_{geom}/A_{act}. \quad (1)$$

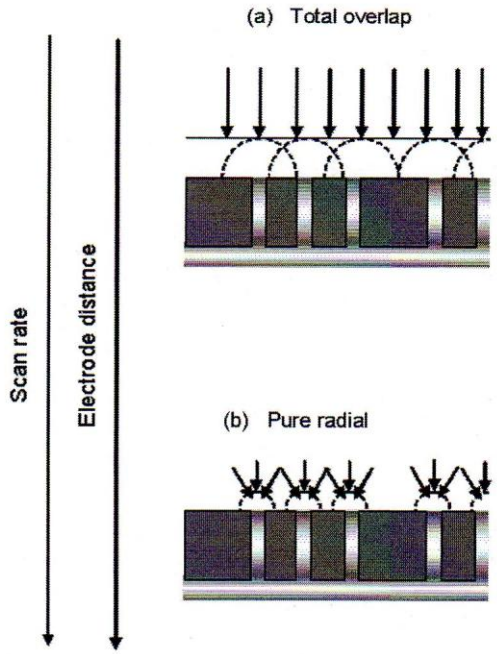

Figure 1. Schematic drawing of the typical diffusive regimes observed at nanoelectrode ensembles as a function of the scan rate and/or nanoelectrodes distance. (a) Total overlap regime; (b) Pure radial regime.

This ratio at the NEE is higher than the relevant ratio at a conventional electrode of the same geometric area for a proportionality factor that is the reciprocal of the fractional electrode area (f) defined as

$$f = A_{act}/A_{geom}. \quad (2)$$

Typical f values for NEEs are between 10^{-3} and 10^{-2}. Faradaic currents at NEEs are equal to those recorded at macroelectrodes of the same geometric area, however at NEEs background currents are dramatically lowered. Such an improvement in the Faradaic to capacitive currents ratio explains why detection limits (DLs) at NEEs can be from 1 to 3 orders of magnitude lower than with conventional electrodes [17,21,29].

3.2 *Cyclic voltammetry of iodide in tap water*

Figure 2, full lines, compares the cyclic voltammograms recorded at an Au-disk electrode in tap water acidified with sulfuric acid, pH 1.0, spiked with 50 μM iodide (Figure 2a) and at a NEE at ten times lower iodide concentration, that is 5 μM (Figure2b). The CVs are characterised by an oxidation peak with associated return peak both at the Au-disk and at the NEE. Oxidation peak currents scale linearly with the square root of the scan rate (not shown); this evidence agrees with the occurrence of a diffusion controlled process. For NEEs, the peak shape of the voltammogram together with the linear dependence of I_p on $v^{1/2}$ indicate the operativity of the total overlap regime with respect to diffusion of

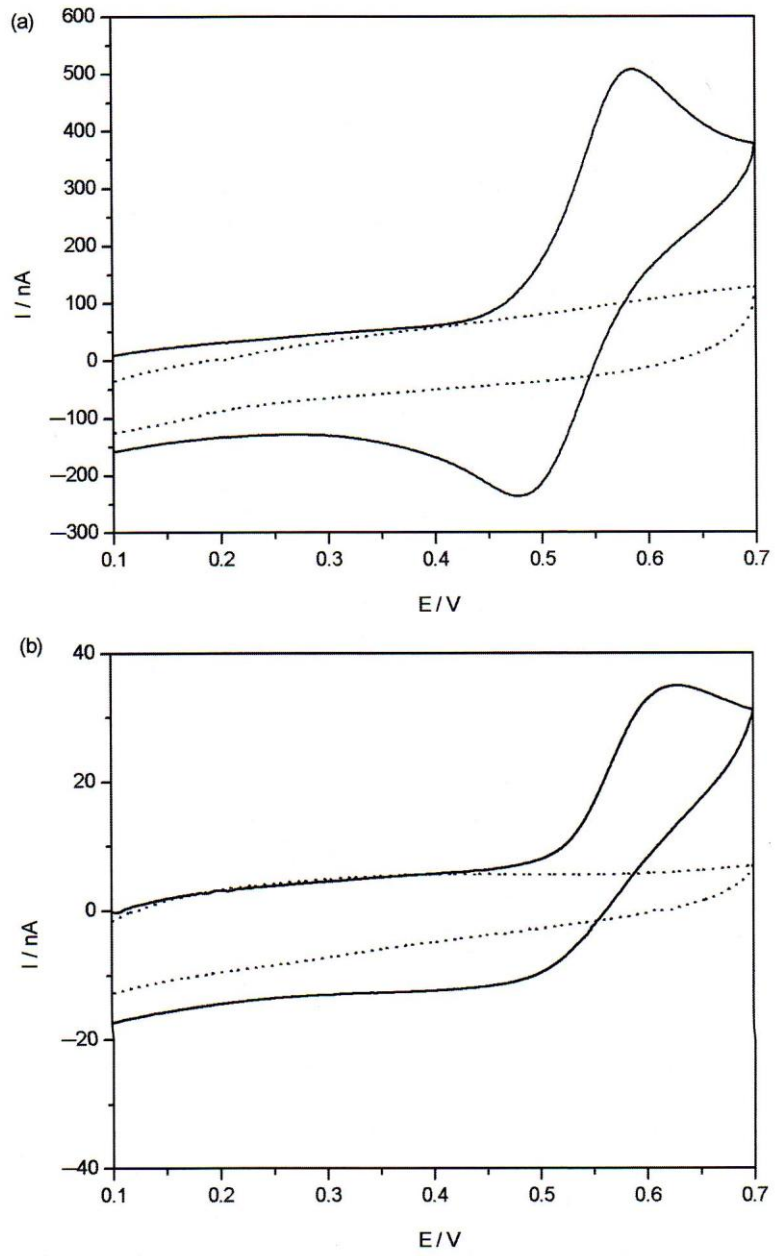

Figure 2. Cyclic voltammograms recorded at 20 m Vs^{-1} in tap water, 0.1 M sulphuric acid solution, pH 1.0, before (·····) and after addition (———) of: (a) 50 μM KI at an Au-disk millimeter-sized electrode; (b) 5 μM KI at a NEE.

iodide to the ensemble of nanoelectrodes. $E_{1/2}$ values, calculated as $(Ep_f + Ep_b)/2$ (where the *f* and *b* subscripts indicate the forward and backward peaks, respectively) were 0.548 V vs. Ag/AgCl at the NEE and 0.524 V vs. Ag/AgCl at the Au-disk. Forward to backward peak separation (ΔEp) values were of the order of 150 mV at the NEE and 80 mV at the

Au macro (both at $20\,mV\,s^{-1}$); these values indicate a quasi-reversible one-electron transfer process, in agreement with previous findings [30]. Note that the kinetic constant for heterogeneous electron transfer, k°, at NEEs is substituted by an apparent constant k°_{app}. NEEs behave indeed as electrodes with partially blocked surface [31] and:

$$k^\circ_{app} = k^\circ f \tag{3}$$

where f is the fractional electrode area. Equation (3) explains the reason why quasi-reversible processes look less reversible at NEEs, as it is observed here for iodide oxidation.

The broken line CVs in the same Figure 2 show the background currents before spiking with iodide, that is in the CV signal relevant to the background electrolyte (blank). As expected, no iodide signal is detected before spiking. The difference in current between the forward (I_f) and backward (I_b) scan in the blank is proportional to the double layer charging current and the electrode area (active area for NEEs) according to the following equation [32,33]:

$$(I_f - I_b) = 2\,vC_{dl}\,A \tag{4}$$

where v is the scan rate, C_{dl} is the double-layer capacitance and A is the metal surface exposed to the solution that is the active area for a NEE and geometric area for an Au-disk electrode. Comparing data for the NEE and the Au-disk electrode, obtained operating under the same experimental conditions and using NEE and Au-disk with the same A_{geom} value, the ratio between background currents results:

$$(I_f - I_b)_{NEE}/(I_f - I_b)_{Au\text{-}disk} = A_{act}/A_{geom} = f. \tag{5}$$

By substituting data obtained from the CVs in Figure 2, measured in correspondence of the $E_{1/2}$ for the I^-/I_2 couple, we can estimate that, for our NEEs, this ratio is 8×10^{-2}. Note that the $E_{1/2}$ of interest is quite positive and not far from the foot of the oxidation limit of the potential window accessible with NEEs in chloride-free solutions [17]. It was demonstrated that for NEEs operating close to this limit, the background current is given not only by the double layer charging current but also by a residual current related to background oxidation [17]. For this reason, the f value can be higher than the value expected only on the basis of geometric considerations (namely 1.3×10^{-2}). Therefore, f value can be considered as an *apparent* fractional electrode area, which, however, should correspond to the real improvement in signal to background current ratio achievable by NEEs, estimated specifically at the potential values where peak currents are really measured.

Focusing on signals recorded at NEEs, the oxidation peak current is directly proportional to the iodide solution concentration and a linear calibration plot is obtained (not shown), with a dynamic range extending over two orders of magnitude and a sensitivity (m, slope of the calibration plot) of $30\,nA\,cm^{-2}\,\mu M$. Current densities are calculated with respect to the overall geometric area of the ensemble. The detection limit DL, calculated as $DL = 3\sigma\,m^{-1}$ (where σ is the standard deviation) resulted $DL = 0.3\,\mu M$. Such a DL is almost one order of magnitude lower than the best literature datum at gold ultramicroelectrodes in water solution [34]. Note also that DL obtained by us at the Au-macro (not shown) is $4\,\mu M$, which is more than one order of magnitude higher than DL at NEEs and the ratio between the two DLs is very close to the f ratio calculated

by Equation (5). We wish to stress that no pre-concentration of the iodide was employed in these analyses.

3.3 *Lagoon water*

The monitoring of iodide and its seasonal cycling in estuarine waters is the subject of specially devoted studies [35,36]; this prompted us to test the use of NEEs for performing the direct determination of iodide in lagoon waters.

Figure 3(a) shows the CVs recorded in a water sample from the lagoon of Venice before and after spiking with standard additions of iodide. The sample was acidified to pH 1 by adding a few drops of concentrated H_2SO_4. The first line CV refers to the sample, while the following ones to the sample spiked with known amount of iodide. The voltammetric oxidation of I^- is less reversible than in the synthetic samples [23] since the forward to backward peak separation increases to 280 mV; however, an oxidation peak is detected, whose current increases with the standard additions. The lower electrochemical reversibility of the CVs is probably due to other components such as organics or surfactants which can be present in this kind of rather raw sample, which underwent only filtration and acidification as pre-treatment. The iodide voltammetric behaviour, particularly the one observed after spiking, is very similar to the one observed previously in table salt samples [23]. The standard addition plot reported in Figure 3(b), allowed us to estimate a I^- concentration in the sample of $(1.6 \pm 0.5)\,\mu M$ i.e. $(203 \pm 63)\,\mu g\,L^{-1}$ for triplicate analysis. Interestingly, this concentration value is slightly higher than the detection limit with NEEs, but lower than DL with millimetre-sized Au-disk electrodes (namely 4 μM [23]). The concentration determined by us in the studied sample compares with literature data from other marine areas [37], however, it is significantly higher than values measured by chromatography in the Venice Lagoon [38], that were between 14 and $32\,\mu g\,L^{-1}$. Both the high standard deviation (31%) and the large difference with previous results from the same area prompted us to improve the determination, lowering the detection limit which, for CV, is too close to the concentration to be determined. It was recently shown that DLs achievable with NEEs can be improved by using pulsed voltammetric techniques instead of CV [19]. Preliminary experiments indicated that square wave voltammetry (SWV) at low frequency is suitable to the goal of determining trace iodide in lagoon waters. Figure 4(a) shows the SW voltammograms recorded in acidified lagoon water before and after spiking with KI. A resolved although rather small peak is detected in the sample with $Ep = 600$ mV vs. Ag/AgCl. It was observed that both the peak height and resolution (given by the ratio $I_p/W_{1/2}$, where $W_{1/2}$ is the half-peak width) reach their maximum at low frequencies, namely 2 Hz. This is explained by the geometry of NEEs and on the time dependence of diffusion layers (see Figure 1). At low time scales, that is at low frequencies, diffusion hemispheres around each nanoelectrode are larger, so that the total overlap condition is achieved. Note that under total overlap conditions, the 100% of A_{geom} contributes to the voltammetric signal [20,33], so that signals are higher than under partial overlap conditions. Another feature evident from the SWVs in Figure 4(a) is the anticipation of the anodic limit of the accessible potential window to 0.700–0.720 V vs. Ag/AgCl (compare, for example, with Figure 2). This is probably related to the easier oxidation of the gold nanoelectrodes caused by the high chloride concentration (0.58 M) present in the sample. Figure 4(b) shows the standard additions plot from which the iodide concentration in the sample is evaluated to be $(0.30 \pm 0.05)\,\mu M$

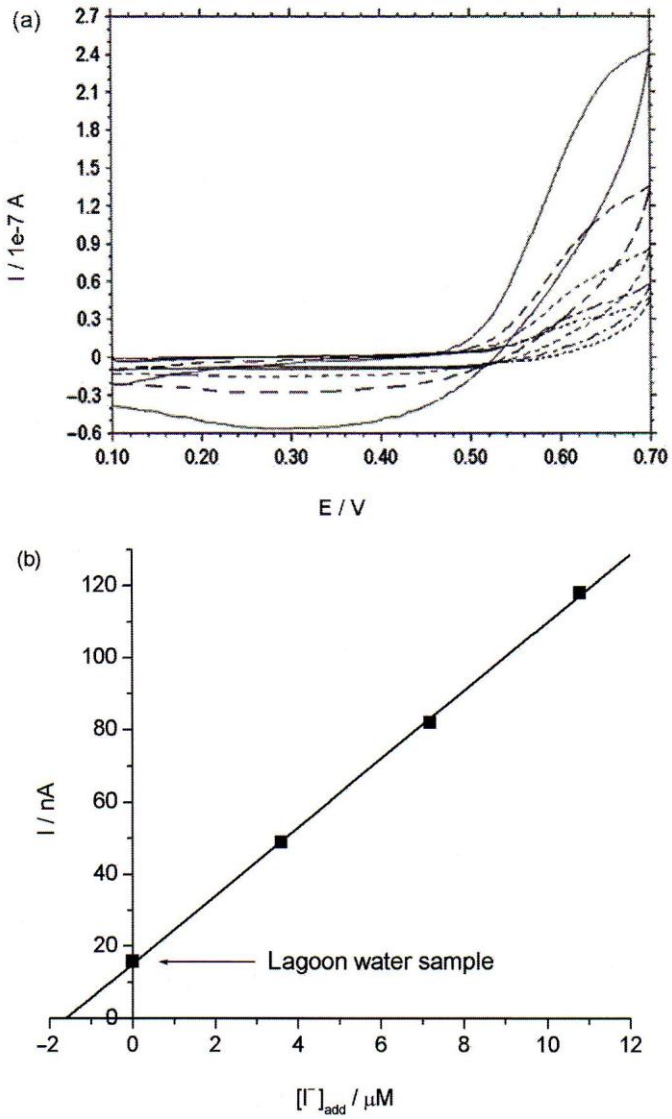

Figure 3. (a) Cyclic voltammograms recorded at 20 m Vs^{-1} at a NEE in lagoon water acidified with sulphuric acid, pH 1.0, before (·····) and after standard additions of KI: 4 μM (– ·–· –), 8 μM (- - -), 12 μM (— — —) and 24 μM (——). (b) Standard additions plot.

for triplicate determinations. Detection limits calculated on the basis of $3\sigma m^{-1}$ criterion, result 0.10 μM and the quantification limit $QL = 10\sigma m^{-1} = 0.30$ μM. Therefore, the concentration determined by us is higher than DL, but close to QL.

As a comparison, the same sample was analysed using the cathodic stripping method at the HMDE after addition of Triton-X 100, proposed by Luther and co-workers [13]. Figure 5 shows the voltammetric pattern and the standard additions plot at the HMDE. The concentration determined resulted (0.40 ± 0.05) μM, that is in agreement with the value measured with the NEE by SWV. Note that with NEE no pre-concentration

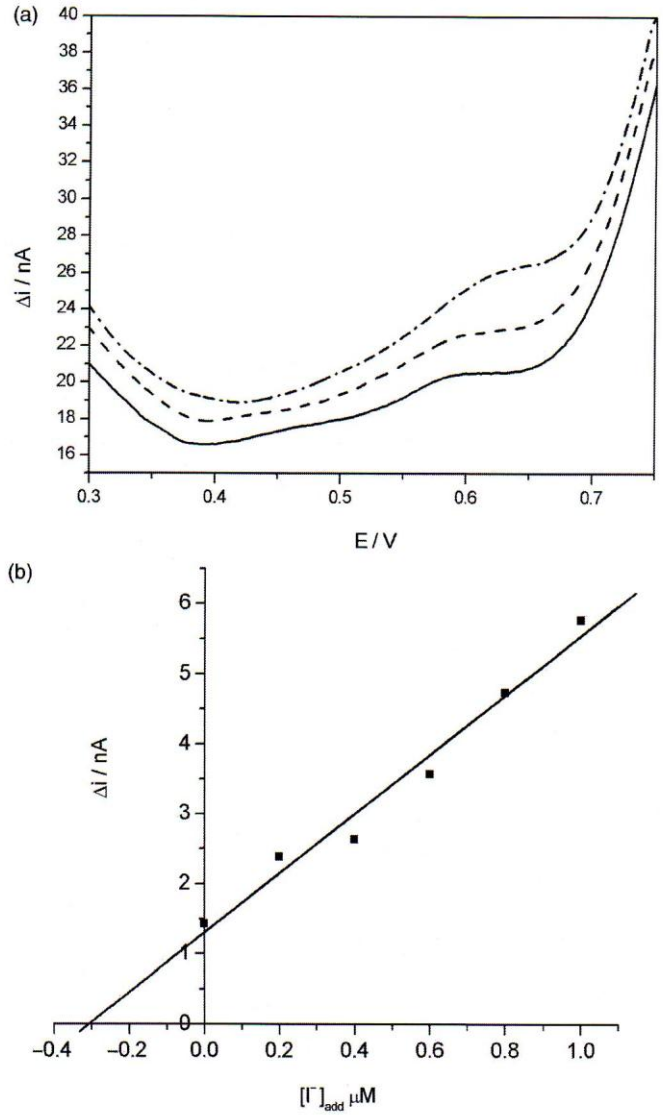

Figure 4. (a) Square wave voltammograms recorded at a NEE in lagoon water acidified with sulphuric acid, pH 1.0, (——) and spiked with 0.4 μM KI (- - -) and 0.8 μM KI (— · — · —). Scan parameters: pulse height 50 mV, frequency 2 Hz. (b) Standard additions plot.

nor deoxygenation of the sample is required, while for cathodic stripping a 180 s pre-concentration and deoxygenation of the sample for several minutes are necessary. However, peak current at the HMDE are better resolved and, indeed, detection limits can, in principle, be further lowered by increasing the pre-concentration time.

4. Conclusions

Nanoelectrode ensembles are advanced nanotech electrochemical sensors which allows one to achieve low detection limits for the direct determination of iodide in water samples.

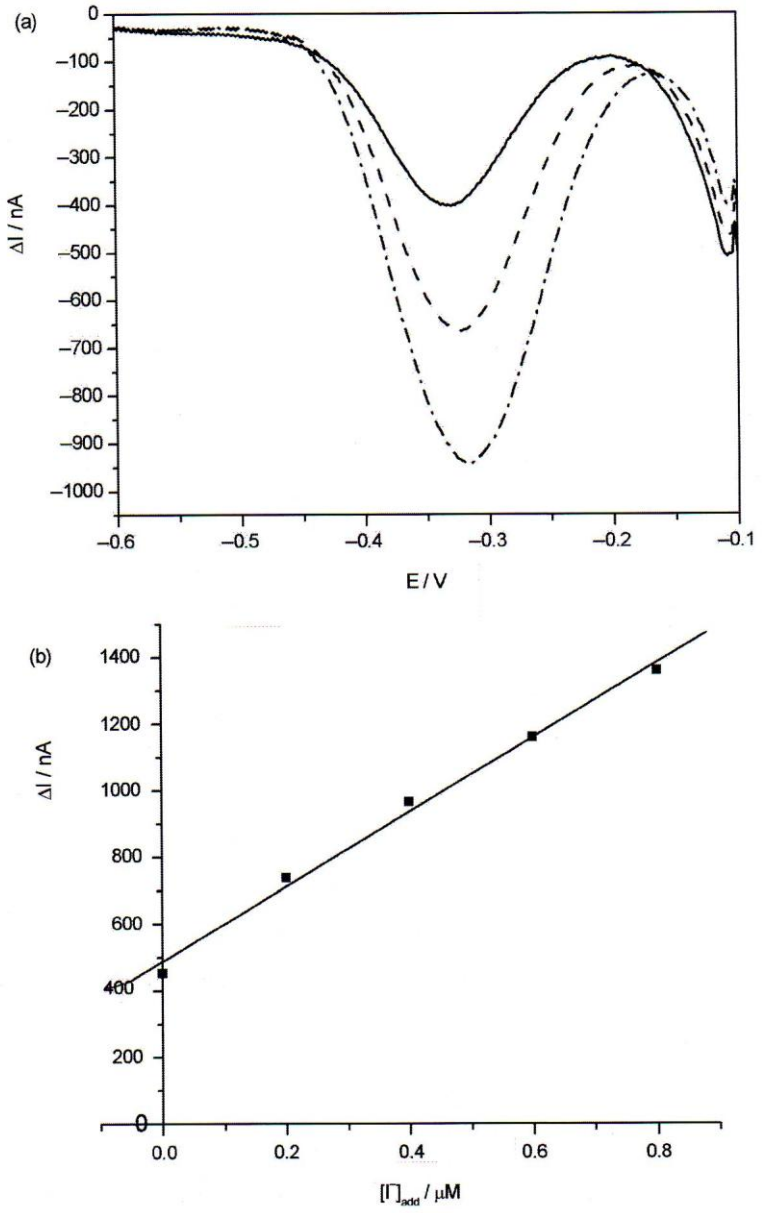

Figure 5. (a) Cathodic stripping square wave voltammograms recorded with a HMDE in lagoon water after the addition of Triton-X 100 (—) and spiked with 0.2 μM KI (- - -) and 0.4 μM KI (— · — · —). Scan parameters: pulse height 20 mV, frequency 100 Hz, deposition time 180 s at −0.1 V. (b) Standard additions plot.

Iodide is oxidised electrochemically both at gold macroelectrodes and at ensembles of gold nanodisks electrode; detection limits at NEEs are one order of magnitude improved with respect to DLs at Au-macroelectrodes. The results presented here show that the use of gold NEEs allows indeed the direct determination of micromolar concentrations of iodide in

water samples. In lagoon waters, a shortening of the potential window accessible makes somehow critical the determination when iodide concentration is in the submicromolar range. Under these conditions, the use of square wave voltammetry improves the detection capabilities. The comparison of the NEE-based method with literature methods at the HMDE [13] indicates that the latter is to be preferred when electrolytic pre-concentration and deoxygenation of the sample are possible, while NEEs are to be preferred when the direct detection is required, and in samples where the iodide concentration is $>0.30\,\mu M$.

Acknowledgements

Financial support by MIUR/Rome is gratefully acknowledged. We thank Dr Manuela De Leo for some preliminary experiments.

References

[1] G.T.F. Wong, Rev. Aq. Sc. **4**, 45 (1991).
[2] P. Pongpaew, S. Saowakontha, R. Tungtrongchitr, U. Mahaweerawat, and F.P. Schelp, Nutr. Res. **22**, 137 (2002).
[3] F. Delange, B. de Benoist, and D. Alnwick, Thyroid **11**, 437 (2001).
[4] J.L. Lambert, G.L. Hatch, and B. Mosier, Anal. Chem. **47**, 915 (1975).
[5] M. Haldimann, B. Zimmerh, C. Als, and H. Gerber, Clin. Chem. **44**, 817 (1998).
[6] K. Ito, T. Ichihara, H. Zhuo, K. Kumamoto, A.R. Timerbaev, and T. Hirokawa, Anal. Chim. Acta **497**, 67 (2003).
[7] K. Yokota, K. Fukushi, S. Takeda, and S.I. Wakida, J. Chromatogr. A **1005**, 145 (2004).
[8] G.T.F. Wong and P.G. Brewer, Anal. Chim. Acta **81**, 81 (1976).
[9] K. Ito, J. Chromatogr. A **830**, 211 (1999).
[10] L. Rong and T. Takeuchi, J. Chromatogr. A **1042**, 131 (2004).
[11] J.P. Perchard, M. Buvet, and K. Molina, J. Electroanal. Chem. **14**, 57 (1967).
[12] K.Z. Brainina and Z. Fresenius, Anal. Chem. **312**, 428 (1982).
[13] G.W. Luther, C.B. Swartz, and W.J. Ullman, Anal. Chem. **60**, 1721 (1988).
[14] R.D. Rocklin and E.L. Johnson, Anal. Chem. **55**, 4 (1983).
[15] I. Svancara, J. Konvalina, K. Schachl, K. Kalcher, and K. Vytras, Electroanalysis **10**, 435 (1998).
[16] A. Walcarius, G. Lefevre, J.P. Rapin, G. Renaudin, and M. Francois, Electroanalysis **13**, 313 (2001).
[17] B. Brunetti, P. Ugo, L.M. Moretto, and C.R. Martin, J. Electroanal. Chem. **491**, 166 (2000).
[18] P. Ugo, N. Pepe, L.M. Moretto, and M. Battagliarin, J. Electroanal. Chem. **560**, 51 (2003).
[19] L.M. Moretto, N. Pepe, and P. Ugo, Talanta **62**, 1055 (2003).
[20] P. Ugo, L.M. Moretto, and F. Vezzà, Chem. Phys. Chem. **3**, 917 (2002).
[21] V.P. Menon and C.R. Martin, Anal. Chem. **67**, 1920 (1995).
[22] W. Vastarella, L. Della Seta, A. Masci, J. Maly, M. De Leo, L.M. Moretto, and R. Pilloton, Intern. J. Environ. Anal. Chem. **87**, 701 (2007).
[23] F.C. Pereira, L.M. Moretto, M. De Leo, M.V.B. Zanoni, and P. Ugo, Anal. Chim. Acta **575**, 16 (2006).
[24] M. De Leo, F.C. Pereira, L.M. Moretto, P. Scopece, S. Polizzi, and P. Ugo, Chem. Mater. **19**, 5955 (2007).
[25] M. De Leo, A. Kuhn, and P. Ugo, Electroanalysis **19**, 227 (2007).
[26] H.J. Lee, C. Beriet, R. Ferrigno, and H.H. Girault, J. Electroanal. Chem. **502**, 138 (2001).
[27] J.C. Hulteen, V.P. Menon, and C.R. Martin, J. Chem. Soc. Faraday Trans. **92**, 4029 (1996).
[28] M. De Leo, L.M. Moretto, O. Buriez, and P. Ugo, Electroanalysis **21**, 392 (2009).

[29] P. Ugo, L.M. Moretto, S. Bellomi, V.P. Menon, and C.R. Martin, Anal. Chem. **68**, 4160 (1996).
[30] M.A. Tadayyoni, P. Gao, and M.J. Weaver, J. Electroanal. Chem. **198**, 125 (1986).
[31] C. Amatore, J.M. Saveant, and D. Tessier, J. Electroanal. Chem. **147**, 39 (1983).
[32] A.J. Bard and L. Faulkner, *Electrochemical Methods* (Wiley, New York, 2000), p. 18.
[33] P. Ugo and L.M. Moretto, in *Handbook of Electrochemistry*, edited by C. Zoski (Elsevier, Amsterdam, 2007), Chap. 16.2.
[34] W. Zhang, H. Zha, B. Yao, C. Zhang, X. Zhou, and S. Zhong, Talanta **46**, 711 (1998).
[35] G.W. Luther III and H. Cole, Mar. Chem. **24**, 315 (1988).
[36] G.T.F. Wong and L.-S. Zhang, Est. Coast. Shelf Sc. **56**, 1093 (2003).
[37] L. Rong, L.W. Lim, and T. Takeuchi, Talanta **72**, 1625 (2007).
[38] E. Marengo, M.C. Gennaro, D. Giacosa, C. Abrigo, G. Saini, and M.T. Avignone, Anal. Chim. Acta **317**, 53 (1995).